

Enhancement of spontaneous emission in a quantum well by resonant surface plasmon coupling

Arup Neogi, Chang-Won Lee, and Henry O. Everitt*
Department of Physics, Duke University, Durham, NC 27708, USA

Takamasa Kuroda and Atsushi Tackeuchi
Department of Applied Physics, Waseda University, Okubo 3-4-1, Shinjuku, Tokyo 169-8555, Japan

Eli Yablonovitch
Department of Electrical Engineering, University of California, Los Angeles, CA 90095, USA
 (Dated: October 29, 2018)

Using time-resolved photoluminescence measurements, the recombination rate in an $\text{In}_{0.18}\text{Ga}_{0.82}\text{N}/\text{GaN}$ quantum well (QW) is shown to be greatly enhanced when spontaneous emission is resonantly coupled to a silver surface plasmon. The rate of enhanced spontaneous emission into the surface plasmon was as much as 92 times faster than normal QW spontaneous emission. A calculation, based on Fermi's golden rule, reveals the enhancement is very sensitive to silver thickness and indicates even greater enhancements are possible for QWs placed closer to the surface metal coating.

The spontaneous emission (SE) decay constant τ for radiating dipoles at \vec{r}_e is given by Fermi's golden rule

$$\frac{1}{\tau} = \frac{2\pi}{\hbar} |\langle f | \vec{d} \cdot \vec{E}(\vec{r}_e) | i \rangle|^2 \rho(\hbar\omega), \quad (1)$$

where $\rho(\hbar\omega)$ is the photon density of states (DOS) and $\langle f | \vec{d} \cdot \vec{E}(\vec{r}_e) | i \rangle$ is the dipole emission matrix element. As pointed out by Purcell, SE may be enhanced by altering the photon DOS¹. For example, the ratio of enhanced to free space emission (the Purcell factor F) has been measured as large as 5 in an atomic system by placing the radiating atoms in a high Q , low volume cavity^{2,3}. A Purcell factor of up to 6 has been observed from quantum well (QW) and quantum dot emitters in vertical cavity surface emitting laser structures, while an enhancement of 15 has been observed from quantum dots in a microdisk cavity^{4,5}. Photonic crystals and distributed Bragg gratings have also been used to enhance the SE rate by as much as a factor of 4.5^{6,7,8}. Such enhanced SE rates, achieved by increasing the photonic DOS in a small cavity, permit lower threshold, higher modulation frequency lasers as well as more efficient light emitting diodes.

The SE rate can also be modified when semiconductor or dye emitters are coupled to a surface plasmon (SP) of a metallic film^{9,10,11,12}. A single QW can experience strong quantum electrodynamic coupling to a SP mode if placed within the SP fringing field penetration depth. An electron-hole pair in the QW recombines and emits a photon into a SP mode instead of into free space. The degree of SE rate modification for a given wavelength depends on the SP DOS at that wavelength. The strongest enhancement occurs near the asymptotic limit of the SP dispersion branch, the SP "resonance" energy E_{sp} , where the SP DOS is very high. Non-resonant, SP-mediated SE enhancements as large as 6 have been observed from GaAs QWs near thin Ag films⁹. Even greater

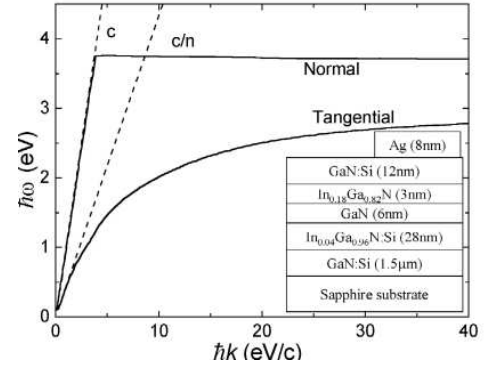


FIG. 1: The calculated surface plasmon dispersion relation for tangential and normal modes. Inset: The structure of the sample studied.

enhancements are possible for wide bandgap semiconductors whose emission wavelength is coincident with E_{sp} . In this report, time-resolved photoluminescence (TRPL) measurements of a partially silver-coated InGaN/GaN QW directly demonstrate the SP-mediated resonant enhancement of the SE rate for the first time in a semiconductor QW.

An InGaN/GaN QW was used in these experiments, grown by metal-organic chemical vapor deposition (MOCVD) on sapphire substrate¹³. Over a 1.5 μm Si-doped GaN buffer layer was grown a 28 nm $\text{In}_{0.04}\text{Ga}_{0.96}\text{N}$ reference layer, a 6 nm GaN layer, and the 3 nm $\text{In}_{0.18}\text{Ga}_{0.82}\text{N}$ QW as shown in Fig. 1. Above the QW was a 12 nm Si-doped GaN cap layer, placing the QW within the fringing field depth of the SP. A layer of silver, ~ 8 nm thick, was deposited by electron beam evaporation on one-half of the sample surface. The other half was left bare to facilitate direct comparison of the silvered and unsilvered results.

The bulk plasmon energy of silver is 3.76 eV, but

the SP energy of Ag is lowered by the GaN dielectric constant¹⁴. The SP dispersion relation is derived, using Maxwell's equations, from the known dielectric properties of Ag and GaN¹⁵. Considering a silver film of thickness t and permittivity ε_2 , sandwiched between GaN and air with permittivities ε_1 and ε_3 respectively, the boundary condition gives the SP dispersion relation

$$\left(\frac{\gamma_1}{\varepsilon_1} + \frac{\gamma_2}{\varepsilon_2}\right)\left(\frac{\gamma_3}{\varepsilon_3} + \frac{\gamma_2}{\varepsilon_2}\right) - \left(\frac{\gamma_1}{\varepsilon_1} - \frac{\gamma_2}{\varepsilon_2}\right)\left(\frac{\gamma_3}{\varepsilon_3} - \frac{\gamma_2}{\varepsilon_2}\right)e^{-2\gamma_2 t} = 0, \quad (2)$$

where $\gamma_i = k^2 - \varepsilon_i \omega^2 / c^2$, $i = 1, 2, 3$, and $k = 2\pi/\lambda$ is the wavevector. The SP dispersion contains tangential and normal mode branches (Fig. 1), indicating the dominant direction of current flow in the silver film. For silver films with $t \geq 8$ nm, the tangential SP branch asymptotically approaches $E_{sp} = 2.85$ eV ($\lambda_{sp} = 436$ nm), the SP "resonance" energy. Because the photon DOS is proportional to $dk/d\omega$, the SP DOS and SE enhancement will be greatest at the SP resonance.

The resonant enhancement is measured by comparing the luminescence decay rate from the photoexcited QW on the silvered and unsilvered sides. Room temperature TRPL measurements were performed using a 100 MHz Kerr-lens mode-locked, frequency-doubled Ti:Sapphire(Ti:S) laser with average incident pump power of 10 mW ($\sim 13 \mu\text{J}/\text{cm}^2$). The pump excitation energy (3.14 eV or 395 nm) was chosen to be below the bandgap of the InGaN reference layer and GaN layers so electron-hole pairs were generated only in the QW. The luminescence signal was dispersed in a grating spectrometer (600 gr/mm) and measured simultaneously across three wavelength bands (2.55-2.68, 2.71-2.87, and 2.79-2.96 eV) using a Hamamatsu streak camera with a resolution of 15 ps. The three adjacent 25 nm (~ 150 meV) wide wavelength bands spanned the entire continuous wave photoluminescence (cw PL) emitted from the QW. Features narrower than 25 nm were resolved by sequentially comparing adjacent 5 or 10 nm data windows offset from each other in 1 - 4 nm steps. Of course, all TRPL traces represent the sum effect of components with wavelength dependent behavior. However, narrowing the bandwidth of the windows further did not significantly improve the ability to measure wavelength dependence because of the reduced signal-to-noise, especially on the silvered side.

An example of a TRPL trace is presented in Fig. 2a, comparing the temporal decay of the unsilvered and silvered QW PL for a 25 nm-wide wavelength band. The luminescence decay constants from the silvered and unsilvered sides were independently derived from exponential fits to the data (5 or 10 nm windows) and then compared under identical pump and detector parameters. The uncertainty in fitted rate constants for a 10 nm window is 2 - 5 % at wavelengths near the peak cw PL emission (2.75 eV) and rises to as much as 10 - 16 % at longer and shorter wavelength extremes where the emission is weaker.

On the unsilvered side, the QW exhibited a long single

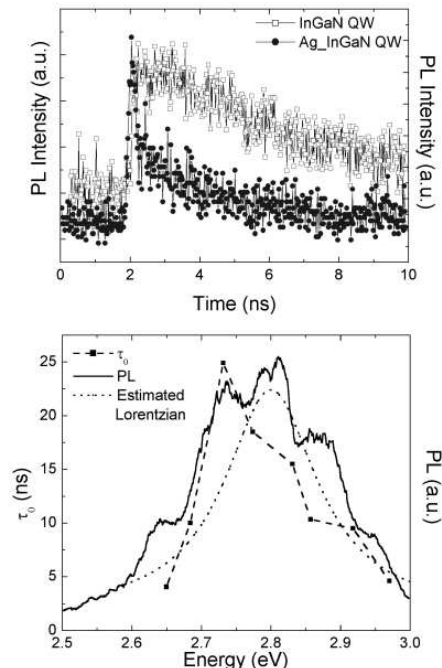


FIG. 2: a) TRPL decay of the unsilvered and silvered InGaN QW for a 25 nm-wide wavelength detection window (2.79-2.96 eV), with pump energy of 3.14 eV. b) Comparison of the cw PL and the TRPL-measured recombination rate constant (τ_0) of the unsilvered InGaN QW. The dashed curve is the estimation given by (4) with $\hbar\omega_c = 2.8$ eV and $\hbar\Delta\omega = 0.16$ eV.

exponential decay whose decay constant τ_0 was slowest ($\tau_0 = 28$ ns) at wavelengths near the peak PL emission (2.76 eV) (Fig. 2b). This very long decay constant, and the correspondingly high PL intensity, indicate a high internal quantum efficiency and insignificant non-radiative (nr) processes compared to radiative (r) recombination ($1/\tau_0 = 1/\tau_{nr} + 1/\tau_r \simeq 1/\tau_r$)^{16,17}. Away from the peak PL emission wavelength, the recombination rate accelerates ($\tau_0 = 4 - 5$ ns) at the longest and shortest wavelengths measured. The wavelength dependence of QW emission is well understood from earlier TRPL studies of InGaN QWs¹⁷ but differs markedly from the SE rate of a dipole radiator (dipole moment d) in a dielectric medium (index of refraction n)

$$\frac{1}{\tau_r(\omega)} = \frac{4nd^2\omega^3}{3\hbar c^3}, \quad (3)$$

especially at low frequency where shallow level traps, impurities, and quantum dot-like structures in the QW contribute to recombination. A phenomenological estimate is a Lorentzian

$$\frac{1}{\tau_0(\omega)} \simeq \frac{1}{\tau_r(\omega)} = \frac{1}{\tau_{r0}} \frac{\Delta\omega^2}{(\omega - \omega_c)^2 + \Delta\omega^2}, \quad (4)$$

whose peak at (ω_c) and linewidth $\Delta\omega$ also roughly coincide with that of the measured cw PL (Fig. 2b).

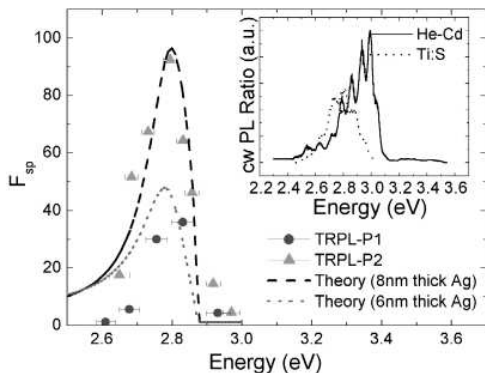


FIG. 3: The Purcell enhancement factor, F_{sp} , measured using TRPL windows 10nm (position P_1) and 5nm (position P_2) wide. Overlaid is the prediction of the enhancement. Inset: Comparison of the time-integrated PL emission ratios for excitation by HeCd and Ti:S lasers.

By contrast, the weaker PL intensity through the silver-coated surface exhibits a bi-exponential decay. The faster decay component, with decay constant τ_1 , corresponds to enhanced recombination mediated by the SP mode ($1/\tau_1 = 1/\tau_{nr} + 1/\tau_r + 1/\tau_{sp} \simeq 1/\tau_{sp}$). As expected, this faster component is strongest near E_{sp} (2.85 eV), but it is evident at energies 200meV lower than E_{sp} and decays with an almost wavelength-independent constant of $\tau_1 \simeq \tau_{sp} \sim 235$ ps. Evidently, the SP resonance is fairly broad. The slower TRPL relaxation component has a decay constant (τ_2) which decreases with decreasing wavelength from 5 ns at 2.94 eV to 9 ns at 2.61 eV. This component is the remnant radiative relaxation component of the QW (τ_r). The frequency dependence is approximately ω^{-3} as in (3), and the role of other non-radiative processes is not evident.

To summarize the wavelength dependence of the SP enhancement, Fig. 3 plots the Purcell factor ($F_{sp} = 1 + \tau_0/\tau_1$) derived from the measured TRPL decay constants. The data demonstrate a sudden rise at higher energies, a peak enhancement at 2.8 eV, and weaker enhancement at lower energies. The maximum values of F_{sp} were 36 (at 2.83 eV) and 92 (at 2.79 eV) at sample positions P_1 and P_2 , respectively. By comparing the relative cw PL intensities of the InGaN reference layers, it is evident that the silver film is thicker at P_2 than at P_1 . The differing F_{sp} values at P_1 and P_2 consequently suggests a sensitivity of F_{sp} to Ag thickness.

Fermi's golden rule (1) provides insight into the frequency dependence of the Purcell factor and reveals the sensitivity of F_{sp} to the silver thickness t and Ag-QW separation a ¹¹. First, the electric field of the SP mode at the QW must be calculated and used to derive the dipole matrix element. The SP electric field varies only in the z direction, so the normalization of $E(z)$ to a half quantum of zero-point fluctuation in the dispersive medium

becomes

$$\alpha^2 = \frac{S}{A} = \frac{\hbar\omega/2}{\frac{A}{8\pi} \int_{-\infty}^{\infty} dz \frac{\partial(\omega\varepsilon(\omega,z))}{\partial\omega} |E(z)|^2}, \quad (5)$$

where $E(z)$ is the unnormalized electric field at a distance z from the Ag-GaN interface, $|\alpha E(a)|^2$ is the normalized electric field at QW depth a , A is the quantization area, and $\varepsilon(\omega, z)$ is the dielectric function of the GaN, Ag, or air. The enhanced recombination rate ($1/\tau_{sp}$) can then be estimated in the QW under the influence of the local electric field from the tangential SP mode

$$\begin{aligned} \frac{1}{\tau_{sp}(\omega)} &= \frac{2\pi}{\hbar} \left(\frac{1}{3} d^2 |\alpha E(a)|^2 \right) 2\pi k \frac{A}{(2\pi)^2} \frac{dk}{d(\hbar\omega)} \\ &= \frac{S}{3\hbar^2} |dE(a)|^2 k \frac{dk}{d\omega}, \end{aligned} \quad (6)$$

where the factor 1/3 comes from spatial averaging of polarization. Inserting measured values for a (12 nm) and t (8 nm) while using the τ_1 data to fit for d (24 nm), the calculation confirms that τ_{sp} is relatively independent of frequency from 2.6 eV to E_{sp} .

The frequency dependence of F_{sp} derives from (6) and the frequency dependence of the unsilvered QW recombination rate τ_0 (Fig. 2b). For the parameters in this experiment, the frequency dependence of F_{sp} below E_{sp} derives primarily from τ_0 . Unfortunately, a predictive theory of the τ_0 is not available, so an accurate estimate of F_{sp} is not possible. However, if (4) and (6) are used as approximations for τ_0 and τ_1 , respectively, then $F_{sp}(\omega) \simeq 1 + \frac{\tau_0}{\tau_1}$ may be plotted (Fig. 3) using the parameters for this sample. The predicted frequency peak and width of F_{sp} agree well with the measured peaks and widths of the TRPL data. The peak value of F_{sp} is a sensitive function of Ag thickness through τ_{sp} . A reduction of t from 8 to 6 nm halves the peak value of F_{sp} , suggesting that the differing values of F_{sp} observed at P_1 and P_2 arise from small variations of the Ag thickness.

Recently, F_{sp} was measured in a similar sample by means of cw PL using a HeCd excitation source ($E_{ex} = 3.82$ eV, $\lambda_{ex} = 325$ nm)¹¹. A ratio of the PL emission for the unsilvered to silvered sides was measured as a function of wavelength, and a peak enhancement factor of 55 was estimated from the data. Those measurements were repeated here, and although the measured enhancement factors were similar to and consistent with the TRPL data, the energy of maximum enhancement in both cw PL measurements was blue shifted from E_{sp} . When time-integrated PL is measured using the Ti:S laser instead, this blue shift disappears (inset, Fig. 3). Note that the HeCd laser excites all layers of the sample while the Ti:S laser only excites the QW. Therefore, any cw PL ratio measured using a HeCd laser must be understood to represent F_{sp} convolved with other excitation-dependent effects (particularly in the cap layer), while the TRPL data measures only F_{sp} . Furthermore, the role of nonradiative

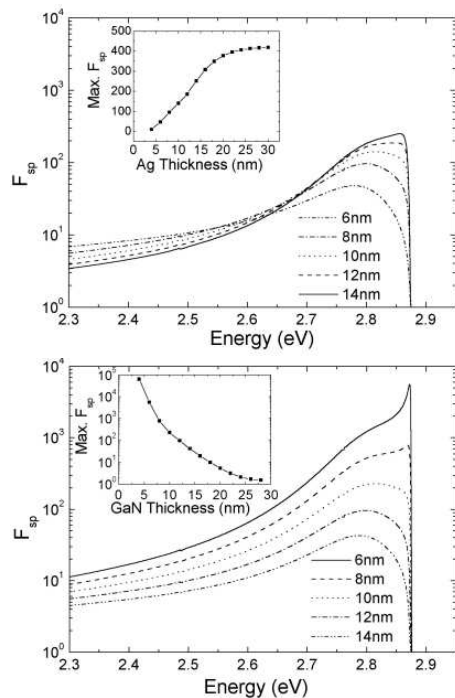


FIG. 4: a) Calculated F_{sp} for various Ag thicknesses t with Ag-QW separation $a = 12$ nm. Inset: Maximum F_{sp} values for a given t with $a = 12$ nm. b) Calculated F_{sp} for various Ag-QW separations a with Ag thickness $t = 8$ nm. Inset: Maximum F_{sp} values for a given a with $t = 8$ nm.

recombination was ignored in that work, leading to an overly simplistic estimate of F_{sp} .

Using (4) and (6) to estimate F_{sp} , even larger enhancements are predicted over narrower frequency bands. For a prominent resonance in F_{sp} , Fig. 4 indicates that it is necessary for the Ag film to possess a thickness ≥ 6 nm for a QW 12 nm from the surface. In support of the earlier deduction that the Ag film is slightly thicker at P_2 than P_1 , the value of F_{sp} is predicted to increase with increasing film thickness and asymptotically approaches 422 for $t \geq 26$ nm ($a = 12$ nm).

The strength and frequency dependence of F_{sp} are even more sensitive functions of the Ag-QW separation, especially for small a . Resonant enhancements of more than 10^4 are predicted for QWs only 4 nm below the surface. These predicted enhancements may actually be conservative because the synergistic "back action" coupling between dipole emitters and SP field, which increases as a decreases, is not included in this calculation. A more comprehensive calculation of this enhancement factor, including the necessary radiation reaction effects, is beyond the scope of this paper. Nevertheless, the enhancement will likely remain broad because inhomogeneous broadening ($\hbar\Delta\omega_{inh} \simeq 100$ meV) will probably limit $\frac{\omega_p}{\Delta\omega} < 30$.

Acknowledgments

The authors would like to thank S. Kellar, U. Mishra, and S. DenBaars of UCSB for providing the QW sample, and I. Gontijo, M. Boroditsky, and G. Khitrova for useful discussions. This work was supported by the Army Research Office and the National Research Council.

* Email address: everitt@aro.arl.army.mil

¹ E. M. Purcell, Phys. Rev. **69**, 681 (1946).

² E. V. Goldstein and P. Meystre, in *Spontaneous Emission and Laser Oscillation in Microcavities*, edited by H. Yokoyama and K. Ujihara (CRC, Boca Raton, 1995), p. 1.

³ S. M. Dutra and P. L. Knight, Phys. Rev. A **53**, 3587 (1996).

⁴ C. Weisbuch, H. Benisty and R. Houdré, J. Lumin. **85**, 271 (2000).

⁵ J. M. Gérard *et al.*, Phys. Rev. Lett. **81**, 1110 (1998); E. Moreau *et al.*, Appl. Phys. Lett. **79**, 2865 (2001).

⁶ J. Vučković, M. Lončar, and A. Scherer, IEEE J. Quantum Elect. **36**, 1131 (2000).

⁷ M. Borditsky *et al.*, J. Lightwave Technol. **17**, 2096 (1999).

⁸ T. Baba *et al.*, J. Lightwave Technol. **17**, 2113 (1999).

⁹ N. E. Hecker *et al.*, Appl. Phys. Lett. **75**, 1577 (1999).

¹⁰ T. Baba *et al.*, Jpn. J. Appl. Phys. **35**, 97 (1996).

¹¹ I. Gontijo *et al.*, Phys. Rev. B **60**, 11564 (1999).

¹² A. Brillante and I. Pockran, J. Mol. Struct. **79**, 169 (1982).

¹³ S. Keller *et al.*, J. Cryst. Growth **195**, 258 (1998) and references therein.

¹⁴ H. Ehrenreich and H. R. Philipp, Phys. Rev. **128**, 1622 (1962); A. Liebsch, Phys. Rev. Lett. **71**, 145 (1993).

¹⁵ G. Hass and L. Hadley, Chap. 6g in *American Institute of Physics Handbook*, 3rd Ed. (McGraw-Hill, New York, 1972), p. 6-149; D. Brunner *et al.*, J. Appl. Phys. **82**, 5090 (1997).

¹⁶ B. Monemar *et al.*, in *Proceedings of SPIE - Ultrafast Phenomena in Semiconductors III* edited by K. T. Tsen, (vol. 3624, 1999), p. 168.

¹⁷ S. F. Chichibu, Y. Kawakami, and T. Sota, Chap. 5 in *Introduction to Nitride Semiconductor blue lasers and light emitting diodes*, edited by S. Nakamura and S. F. Chichibu, (Taylor & Francis, London, 2000), p. 153-270, and references therein.